

Flow Separation in Rocket Nozzles under High Altitude Condition

R. Stark , C. Génin

German Aerospace Center (DLR), Langer Grund, D-74239 Lampoldshausen, Germany

Corresponding Author: ralf.stark@dlr.de

INTRODUCTION

Within a convergent-divergent rocket nozzle the flow can only withstand a certain degree of overexpansion. Beyond this point the boundary layer separates, lifts off the nozzle wall and ambient air is sucked into the remaining separated backflow section of the nozzle. For a given nozzle geometry, the position of the flow separation is a function of the gas properties, the total and the ambient pressure. This flow separation leads to undesired side loads stressing the nozzle, the rocket engine, the launcher structure and the payload. The prediction of the separation position is crucial for rocket engine design and determines the maximum possible nozzle area ratio, a deciding factor for the engine performance.

The separation characteristics of nozzles under sea-level conditions can be easily studied. The altitude operation of a nozzle can be studied at sea-level by adjusting the nozzle pressure ratio p_0/p_a (NPR) to representative values through increasing the total pressure p_0 . This procedure disregards however the ambient density decrease during launcher ascent.

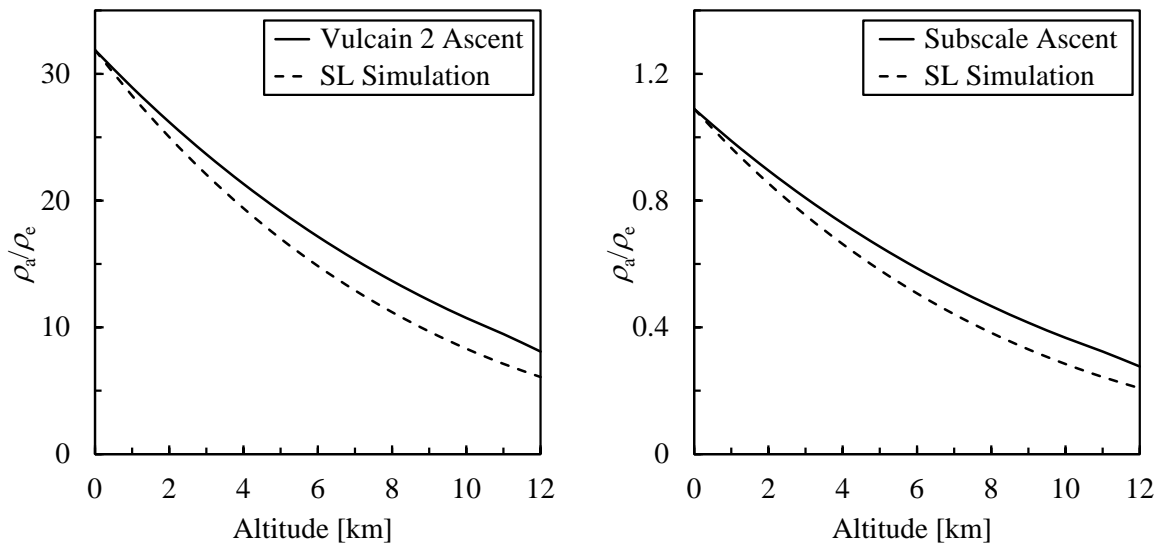


Figure 1: Density ratio Vulcain 2 (left) and cold gas subscale model (right).

Figure 1, left illustrates the effect for the main stage engine Vulcain 2. The ratio of the ambient air versus the hot gas density at the nozzle exit ρ_a/ρ_e is plotted as a function of the altitude. Added is the density ratio that results if the representative altitude NPR is achieved by an increase of total pressure at sea-level. For this case, the density of the hot gas increases while the ambient density remains constant. For increasing simulated altitude the real and simulated ratio differ noticeably. Therefore the study of conventional nozzles that are foreseen to be started up during launcher ascent or altitude adaptive rocket nozzles, like the dual bell nozzle⁽¹⁾ regarding its mode transition characteristics, can lead to inadequate results.

The dual bell nozzle offers a one-time altitude adaption with an increased thrust resulting in a payload gain. Its sea-level to altitude operating mode transition and hence the related flight

altitude of the launcher can be determined using Equation 1⁽¹⁾, where M_e is the wall Mach number of the dual bell extension

$$NPR_{trans} = \frac{1}{M_e} \left(1 + \frac{\gamma-1}{2} M_e^2 \right)^{\frac{\gamma}{\gamma-1}} \quad (1)$$

The equation is based on the following separation criterion^(2,3)

$$\frac{p_{sep}}{p_a} = \frac{1}{M_{sep}} \quad (2)$$

The criterion characterizes the turbulent flow separation in rocket nozzles under sea-level conditions. Therefore the prediction of the dual bell transition NPR might provide inadequate results, as the influence of the ambient density is not taken into account.

Figure 1, right gives the density ratio of a cold gas subscale nozzle like it is typically used at DLR Lampoldshausen. Here, the density ratio is as well inadequately reproduced for high altitudes (NPR values).

The present work studies experimentally the influence of the ambient density on the flow separation in rocket nozzles.

EXPERIMENTAL SETUP

The study was conducted at DLR's altitude simulation test facility P6.2 in Lampoldshausen. Figure 2, left gives the facility flow chart with the high pressure gaseous nitrogen supply storage and the feeding system consisting of automatic valves, filters, pressure reducers, regulation valves and mass flow meters. The feeding system connects the fluid supply with settling chambers that are mounted upstream the altitude chamber and the ejector system. To reduce turbulence the settling chambers are equipped with a set of grids and honeycombs. The tested nozzle specimen is mounted vertically inside the altitude chamber.

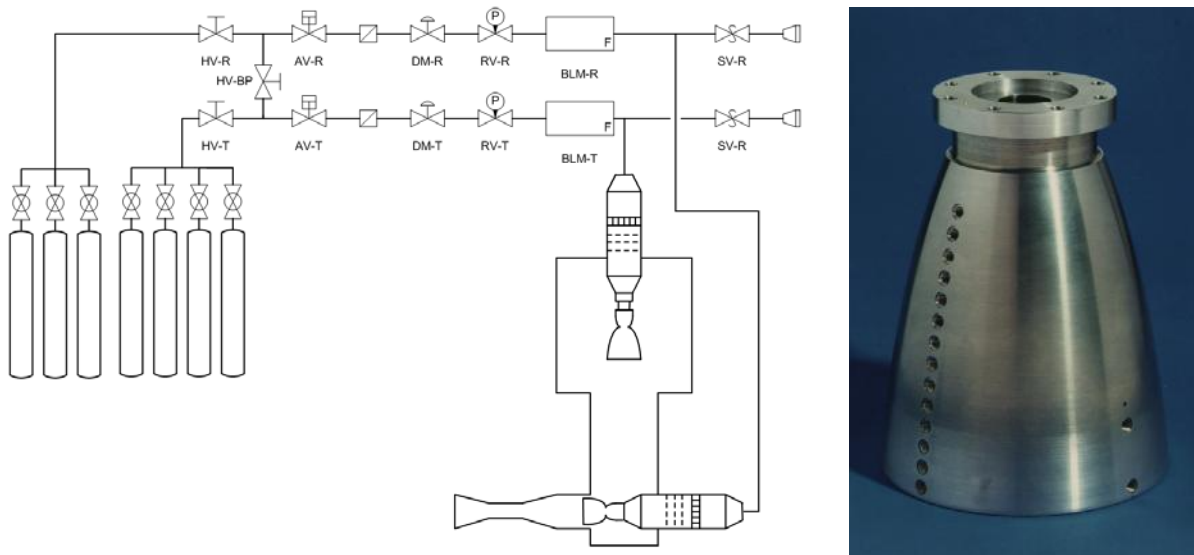


Figure 2: Flow chart of test facility P6.2 (left) and TIC nozzle (right).

The ejector system and the altitude chamber are connected via a guiding tube. The ejector jet evacuates the altitude chamber and mixes with the test specimen exhaust before the complete flow is recompressed by a diffusor. In this way the altitude chamber with the test specimen inside is decoupled from the ambience.

The facility features total pressure up to 60 bars with a mass flow up to 4.2 kg/s. Dry nitrogen is used as working fluid to avoid condensation effects (H₂O, CO₂, O₂, etc.). Its total temperature corresponds to ambience.

TEST SPECIMEN AND PRESSURE MEASUREMENTS

The studied nozzle was a truncated ideal contour nozzle (TIC) with a design Mach number of $Ma_D = 5.15$ and an exit wall Mach number of $Ma_e = 4.4$ (Fig. 2, right). The specimen was made of aluminum. Its wall thickness was 11 mm and the throat radius was $R_{th} = 10$ mm.

The nozzle was equipped with an axial row of 14 wall pressure ports where absolute pressure sensors of Kulite type XT-154-190M were screwed normal into the wall and connected to the flow via small orifices of 0.5 mm diameter. The sensors measuring range were 1 bar with a related accuracy of 0.5 %. The eigenfrequency of their pressure sensitive membrane was 50 kHz. Due to sensor and mounting geometry a filter of 160 Hz was used while the signals were recorded with 1 kHz.

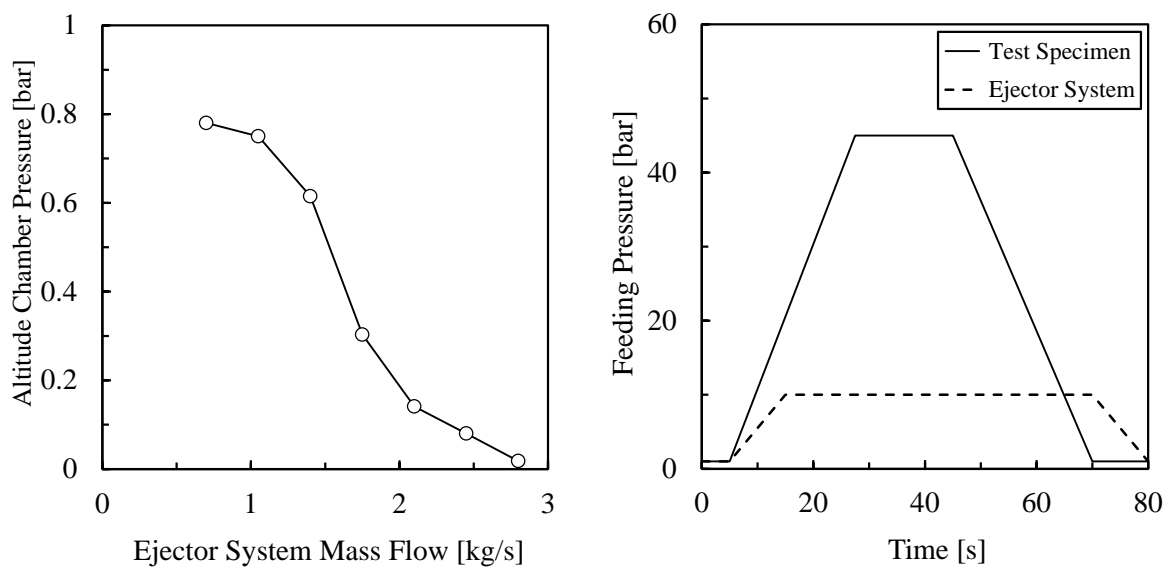


Figure 3: Churn pressure by ejector (left) and test sequence of configuration 1 (right).

TEST PROCEDURE

The tests were conducted for ejector feeding pressures varying from 10 to 35 bars with increments of 5 bars. The mass flow of the ejector system evacuates the altitude chamber. However, ejector mass flow and resulting altitude chamber pressure are not directly proportional. Figure 3, left gives the achievable altitude chamber churn pressure as a function of the ejector mass flow, i.e. without an additional specimen mass flow. Initially, the churn pressure decreases only slightly with increasing ejector mass flow. For ejector mass flows above 1.5 kg/s it decreases rapidly and finally reaches its minimal value for maximum possible ejector mass flow. Table 1 gives the ejector feeding pressure, the related mass flow and the achieved churn pressure for all configurations. The test specimen mass flow increases the altitude chamber pressure to values above the achievable churn pressure.

Figure 3, right depicts a typical test sequence for configuration 1. Initially, the feeding pressures of the TIC nozzle and ejector increase in parallel. The ejector reaches its operating condition before the nozzle. During this up-ramping process the flow separation inside the nozzle moves downstream towards the nozzle exit. For the second half of the sequence the process is reversed, resulting in an upstream move of the separation front. Finally, the ejector system is shut down.

Table 1: Characteristics of ejector system.

	p_0 [bar]	dm/dt [kg/s]	p_{AC} [mbar]
Conf. 1	10	0.7	780
Conf. 2	15	1.05	750
Conf. 3	20	1.4	615
Conf. 4	25	1.75	303
Conf. 5	30	2.1	141
Conf. 6	35	2.45	80

RESULTS and DISCUSSION

The axial position X_{sep} of the flow separation inside the TIC nozzle was determined using the wall pressure measurements. The lowest pressure detected at a sensor position marks the start of the separation zone. This pressure is designated as p_{sep} . Once the orifice of the sensor port lies within the attached supersonic flow region the measured wall pressure p_w is coupled with the total pressure p_0 , i.e. $p_0/p_w = \text{const}$. Using this method it is possible to detect at least the start of the flow separation zone, even if the pressure might be within the sensor lower, nonlinear measuring range and therefore the measured values are no longer reliable.

Figure 4, left compares the evaluated separation positions as a function of the related total to altitude chamber pressure ratio p_0/p_{AC} (NPR). The separation positions are normalized over the nozzle throat radius R_{th} . Configurations 1 to 3 depict a linear relation of separation position and NPR, as known for TIC nozzles under sea-level operation⁽²⁾. Within the back section of the nozzle ($X_{sep}/R_{th} > 6$), for configuration 4 and 5 the separation locations are only attainable with increased NPRs. Here, significant lower pressures and densities are given, for the altitude chamber as well as the nozzle. The data slope of configuration 6 is prominent. Initially, its separation positions are shifted upstream to lower X_{sep}/R_{th} values, recover for a small NPR interval a remarkable distance to finally approach smoothly the nozzle exit and remain upstream the average trend.

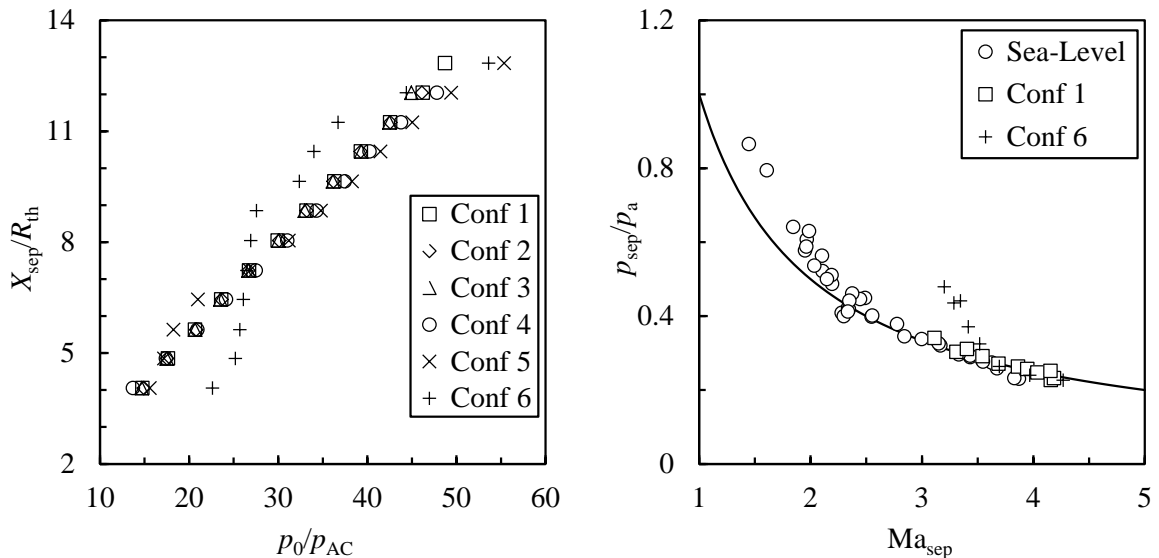


Figure 4: Separation positions (left) and pressures (right), sea-level vs. altitude chamber.

An explanation of this unusual behavior is revealed in Fig. 4, right. Given are the mean separation pressures p_{sep} , normalized over the altitude chamber pressure, as a function of the related wall Mach number Ma_{sep} . The black line depicts the introduced criterion for turbulent separation (eq. 2). The separation pressures achieved with configuration 1 follow the awaited

trend. It is a conventional turbulent flow separation, typical for bell type nozzles under sea-level conditions. In opposite, configuration 6 shows a distinct deviation with a nearly constant gradient for wall Mach numbers below 3.5. Such a behavior is known from previous experimental studies under sea-level conditions, like the comparison with these data (circles) points out. Here, the deviation from the turbulent separation trend is given for wall Mach numbers below 2.4. Former studies showed that this is due to a laminar flow separation^(2, 3). The boundary layer relaminarizes for low total pressures p_0 within the nozzle throat. As the relaminarization is only a function of the total pressure it occurs, if a lower altitude chamber pressure p_{AC} is given, for a higher NPR (p_0/p_{AC}). Consequently, the strong separation position gradient around $p_0/p_{AC} \sim 25$ for configuration 6 in Fig. 4, left indicates the transition from a laminar to a turbulent flow separation.

Figure 5, left gives the mean separation pressures as a function of the related wall Mach number for the other configurations. There is no significant effect of the density ratio, as long as the flow separation is a turbulent one. Therefore, the separation pressure of configuration 5 for wall Mach number $Ma_{sep} = 3.03$ in combination with the related separation data, given in Fig. 4, left, lead to the conclusion that another transition from laminar to turbulent separation was documented.

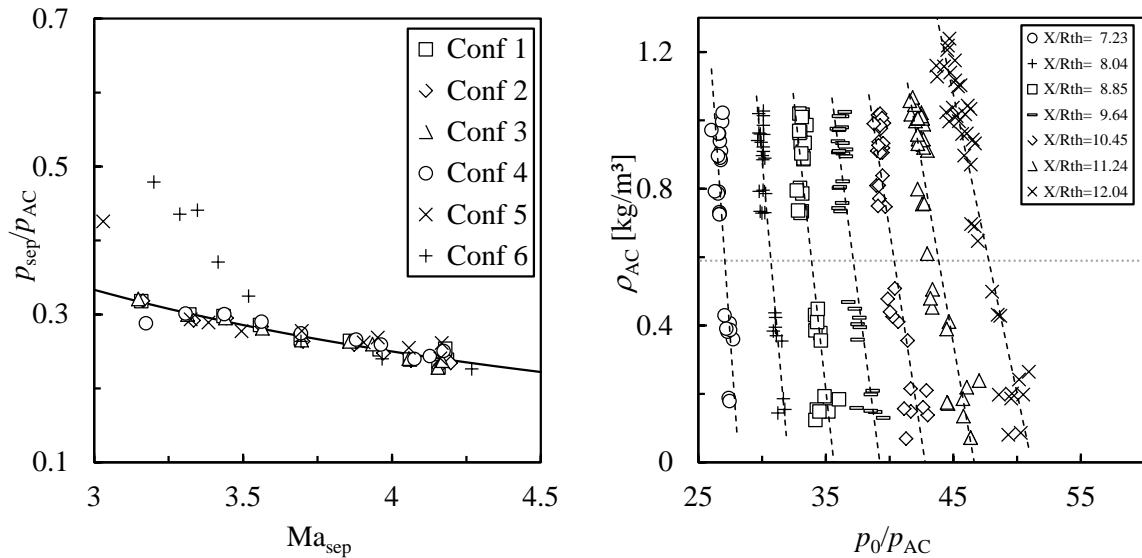


Figure 5: Separation pressures versus wall Mach number (left) and separation as a function of pressure ratio and ambient density (right).

Figure 5, right gives separation data as a function of p_0/p_{AC} (NPR) and ambient density ρ_{AC} . Presented are all conditions where the separation starts at one of seven selected pressure ports. For decreasing ambient density a selected port can only be reached with an increased NPR. The ratio of density decrease and NPR increase can be linearly approximated. If a pressure port lies further downstream the negative gradient of the approximated linear slope increases. With decreasing ambient density the flow separation moves upstream for constant NPR. Figure 6 gives the separation shift gradients as a function of the port positions and the related wall Mach numbers.

The dotted line within Fig. 5, right marks the air density for an altitude of 7 km. In recent system studies⁽⁵⁾ this altitude turned out to be the upper transition mode limit of a dual bell nozzle applied e.g. on Ariane 5 ECA. For densities above the marked value and for separation positions up to $X/R_{th} = 10.45$ the density impact of nozzle flow separation is not significant.

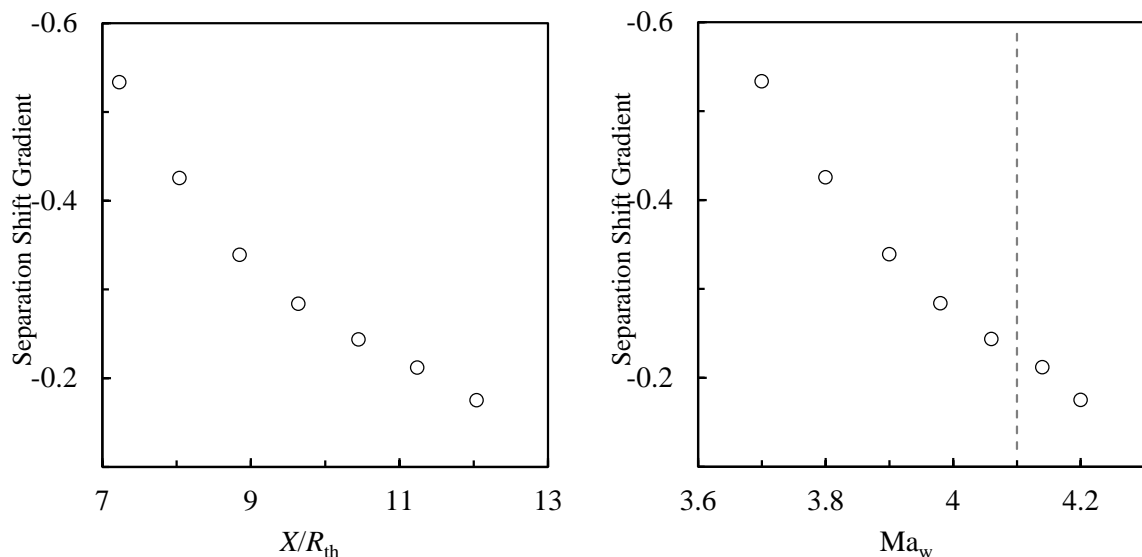


Figure 6: Separation shift gradients as function of axial position (left) and related mean wall Mach number (right).

CONCLUSIONS

It could be shown that the flow separation within rocket nozzles differs for altitude and sea-level conditions. Under altitude conditions the flow separation is shifted upstream. If the NPR of a given flight altitude is simulated with an equivalent sea-level test, the resulting flow separation is in reverse shifted downstream. As the flow separation under altitude conditions is delayed, a dual bell mode transition would take place for an increased NPR compared to a sea-level simulation. A conclusion that is conform to experimental results⁽⁴⁾. It could be shown as well that the observed effect is for realistic dual bell applications of minor significance. The separation criterion (Eq. 2) that was derived from experimental sea-level studies and literature data might have to be adapted for altitudes above 7 km and wall Mach numbers above 4.1.

Furthermore it could be pointed out that laminar flow separation that appears for low total pressures can falsify the separation characteristics, leading to non-representative results. Hence, it is recommended to not adjust the altitude chamber pressure below 300 mbar for flow separation studies.

ACKNOWLEDGEMENTS

The authors would like to thank Prof. Dr. Oskar Haidn and Dr. Shashi Verma for the discussion leading to the presented experimental study.

REFERENCES

1. Génin C. *Experimental Study of Flow Behaviour and Thermal Loads in Dual Bell Nozzles*. Dissertation, Université de Valenciennes, ISBN 978-3-8322-9230-0, (2010).
2. Stark R. *Beitrag zum Verständnis der Strömungsablösung in Raketendüsen* (Contribution to the Understanding of Flow Separation in Rocket Nozzles). Dissertation (in German), RWTH Aachen, (2010).
3. Stark R. and Wagner B. *Experimental study of boundary layer separation in truncated ideal contour nozzles*. Shock Waves, Vol. 19, No. 3, pp 185-191, (2009)
4. Génin C. and Stark R. *Influence of the Test Environment on the Transition of Dual-Bell Nozzles*. 28th ISTS Special Issue, Vol. 10, pp 49-53, (2012)
5. Stark R., Génin C., Schneider D. and Fromm C. *Ariane 5 Performance Optimization using Dual Bell Nozzle Extension*. (2015).